Materials Transactions, Vol. 43, No. 5 (2002) pp. 1230 to 1234

EXPRESS REGULAR ARTICLE

Formation and Soft Magnetic Properties of Co–Fe–Si–B–Nb Bulk Glassy Alloys

Akihisa Inoue and Baolong Shen

Institute for Materials Research, Tohoku University, Sendai 980-8577, Japan

Soft ferromagnetic bulk glassy alloys in Co–Fe–Si–B base system were formed in the diameter range up to 1 mm at the composition of $(Co_{0.705}Fe_{0.045}Si_{0.1}B_{0.15})_{96}Nb_4$ by copper mold casting. Since no bulk glass formation has been obtained in the Co–Fe–Si–B system, the addition of 4%Nb is very effective for the increase in the glass-forming ability. The effectiveness was interpreted by satisfaction of the three component rules for formation of bulk glassy alloys. The bulk glassy alloys exhibit the glass transition before crystallization. The glass transition temperature (T_g), the supercooled liquid region defined by the difference between T_g and crystallization temperature (T_x), ΔT_x ($= T_x - T_g$) and the reduced glass transition temperature (T_g/T_l) are 823 K, 37 K and 0.61, respectively. The bulk glassy alloys also exhibit soft magnetic properties with saturation magnetization (I_s) of about 0.60 T and low coercive force (H_c) below 3 A/m. The synthesis of the Co-based bulk glassy alloy rods with glass transition and good soft magnetic properties is important for future development as a new type of soft magnetic bulk material.

(Received January 31, 2002; Accepted March 25, 2002)

Keywords: *cobalt-based system, bulk glassy alloy, niobium addition, glass transition, reduced glass transition temperature, casting, soft magnetic property*

1. Introduction

In addition to nonferrous metal-based bulk glassy alloys such as lanthanide (Ln)-,[1] Mg-,[2] Zr-,[3,4] Ti-,[5] Pd-,[6] Ni-[7] and Cu-[8] based systems, ferrous group alloys such as Fe-[9] and Co-[10] based systems have been found formed into bulk glassy alloys with diameters ranging from 1 to 6 mm by the copper mold casting method. When we pay attention to the alloy components of Fe- and Co-based bulk glassy alloys, Fe-based systems consist of Fe–(Al, Ga)–(P, C, B),[9] Fe–(Al, Ga)–(P, C, B)–(Nb, Cr, Mo),[11] Fe–Ga–(P, C, B),[12] Fe–Ga-(P, C, B)–(Cr, Nb, Mo),[13,14] Fe–(Zr, Hf, Nb, Ta)–B,[15] Fe–(Zr, Hf, Nb, Ta)–(Mo, W)–B,[16] Fe–Co–Ln–B,[17] Fe–(Nb, Cr, Mo)–(P, B),[18] Fe–(Cr, Mo)–(–B, C),[19] Fe–Ni–P–B[20] and Fe–Si–B–Nb.[21] On the other hand, Co-based bulk glassy alloys are composed of Co–Fe–Ta–B[10] and Co–Fe–Nb–B[22] systems. Here, it is important to point out that all the Fe- and Co-based bulk glassy alloys as well as the nonferrous bulk glassy alloys satisfy the three component rules,[23–25] *i.e.*, (1) multi-component alloy system consisting of more than three elements, (2) significant atomic size mismatches above 12% among the main three constituent elements, and (3) suitable negative heats of mixing among their constituent elements. It has further been clarified that the bulk glassy alloys with the three component rules possess a unique glassy structure with the following features of a higher degree of dense random packed atomic configuration, new local atomic configuration, and long-range homogeneity with attractive interaction.[23–25] The formation of the new glassy structure leads to the retardation of atomic diffusivity as well as the necessity of long-range atomic rearrangements for progress of crystallization, resulting in the formation of bulk glassy alloys through an increase in stability of supercooled liquid against crystallization. Based on the effectiveness of the three component rules, we have searched for a new Co-based bulk glassy alloy with good soft magnetic properties in Co–Fe–Si–B–M (M=Nb or Ta) system which is important as an engineering material. As a result, we have found that bulk glassy alloys are formed in Co–Fe–Si–B–Nb and Co–Fe–Si–B–Ta systems by copper mold casting. This paper presents the compositions at which bulk glassy alloys are formed in Co–Fe–Si–B–Nb system and the thermal stability and magnetic properties of the Co-based bulk glassy alloys and investigates the effect of Nb addition on the increase in the glass-forming ability.

2. Experimental Procedure

Multi-component Co-based alloys with composition of $(Co_{0.705}Fe_{0.045}Si_{0.1}B_{0.15})_{100-x}Nb_x$ ($x = 0$ to 8 at%) were prepared by arc melting the mixtures of pure metals and pure metalloids in an argon atmosphere. The alloy components represent the nominal atomic percentages. Bulk glassy alloy rods with diameters ranging from 0.5 to 2 mm were produced by the copper mold casting method. Melt-spun glassy alloy ribbons with a cross section of $0.02 \times 1.1\,mm^2$ were also produced by the melt spinning technique. The glassy phase was identified by X-ray diffraction and the absence of micrometer scale crystalline phase was examined by optical microscopy (OM). The OM sample was etched for 10 s at room temperature in a solution of 0.5% hydrofluoric acid and 99.5% distilled water. Thermal stability was examined by differential scanning calorimetry (DSC) at heating rates of 0.67 and 1.33 K/s. The melting (T_m) and liquidus (T_l) temperatures were measured by differential thermal analysis (DTA) at heating and cooling rates of 0.33 and 0.033 K/s, respectively. Magnetic properties of saturation magnetization (I_s) and approximate coercive force (H_c) were measured with a vibrating scanning magnetometer (VSM) under an applied field up to 300 kA/m. The accurate coercive force of the melt-spun ribbon alloy was measured by I–H loop tracer under a maximum applied field of 800 A/m.

3. Results

We confirmed the formation of an amorphous single phase without crystallinity in the melt-spun $(Co_{0.705}Fe_{0.045}Si_{0.1}B_{0.15})_{100-x}Nb_x$ ($x = 0$ to 8 at%) alloy ribbons by X-ray diffraction. The result of the Co-based alloy without Nb is consistent with a number of previous data on Co-based amorphous alloys. Figure 1 shows the DSC curves of the amorphous 2%Nb, 4%Nb, 6%Nb and 8%Nb alloy ribbons. It is seen that all the alloys crystallize through two-stage exothermic reactions, though the exothermic peak behavior changes significantly at the Nb compositions between 6 and 8 at%. It is noticed that the glass transition can be observed in the temperature range before crystallization for the 4%Nb, 6%Nb and 8%Nb alloys. The absence of the glass transition for the 2%Nb alloy agrees with the previous result. The glass transition temperature (T_g) and the onset temperature of crystallization (T_x) increase from 823 to 875 K and 860 to 915 K, respectively, with increasing Nb content from 4 to 8 at%. The supercooled liquid region defined by the difference between T_g and T_x also tends to increase from 37 K for the 4%Nb alloy to 40 K for the 8%Nb alloy. With the aim of determining the reduced glass transition temperature (T_g/T_l) which has been thought as one of evaluation parameters for glass-forming ability, we measured the cooling curves of the Nb-containing alloys by DTA at the slow cooling rate of 0.033 K/s. As shown for the DTA curves in Fig. 2, the liquidus temperature (T_l) increases gradually from 1316 to 1370 K in the Nb content between 2 and 4 at% and then significantly to 1358 K for the 6%Nb alloy and 1367 K for the 8%Nb alloy. The resulting T_g/T_l value was evaluated as 0.61 for the 4%Nb alloy, 0.63 for the 6%Nb alloy and 0.64 for the 8%Nb alloy. Figure 3 shows the saturation magnetization (I_s) and coercive force (H_c) as a function of Nb content for the $(Co_{0.705}Fe_{0.045}Si_{0.1}B_{0.15})_{100-x}Nb_x$ amorphous alloy ribbons. As the Nb content increases from 0 to 8 at%, the I_s decreases monotonously from 0.75 T to 0.35 T and the H_c is 1.6 A/m for the 0%Nb alloy, followed by a minimum of 1.5 A/m at 2%Nb and then a monotonous increase to 1.70 A/m. Considering that the 4%Nb alloy exhibits the highest I_s and the lowest H_c for the Co-based amorphous alloys with glass transition, the subsequent search for the formation of a Co-based bulk glassy alloy was made by using the alloy composition of $(Co_{0.705}Fe_{0.045}Si_{0.1}B_{0.15})_{96}Nb_4$.

It was confirmed that the X-ray diffraction patterns of the cast $(Co_{0.705}Fe_{0.045}Si_{0.1}B_{0.15})_{96}Nb_4$ alloy rods consisted only of halo peaks in the diameter range up to 1 mm and the further increase in the rod diameter to 2 mm caused the formation of mixed glassy plus crystalline phases. Figure 4 shows an optical micrograph of the transverse cross section of the cast Co-based alloy rod with a diameter of 1 mm. Although some cavities are observed as small dark spots, no distinct contrast revealing the precipitation of crystalline phase is seen over the whole cross section, indicating the formation of a glassy single phase. Figure 5 shows the DSC curves of the cast Co-based alloy rods with diameters of 0.5 and 1 mm, together with the data of the corresponding melt-spun glassy alloy ribbon. The rod samples exhibit the sequent transition of glass transition, followed by a supercooled liquid region and then two-stage crystallization. We cannot see any appreciable dif-

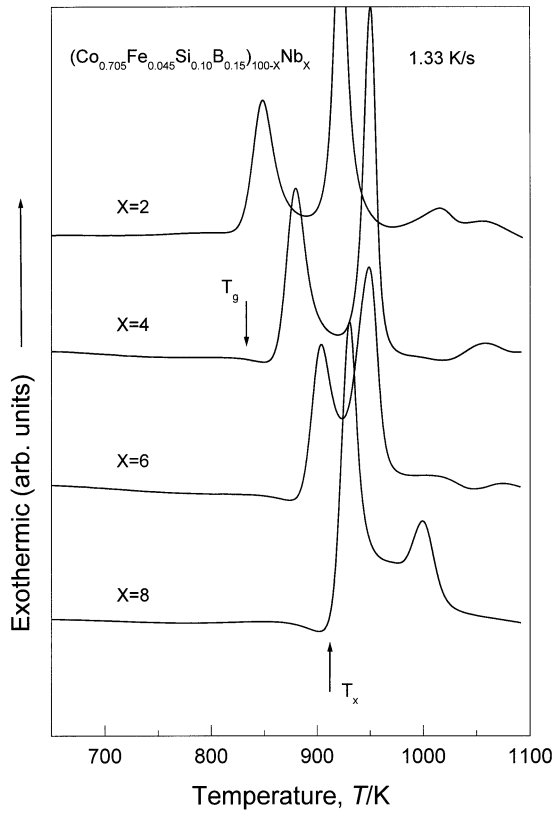

Fig. 1 DSC curves of melt-spun $(Co_{0.705}Fe_{0.045}Si_{0.1}B_{0.15})_{100-x}Nb_x$ ($x = 2$, 4, 6 and 8 at%) amorphous alloy ribbons.

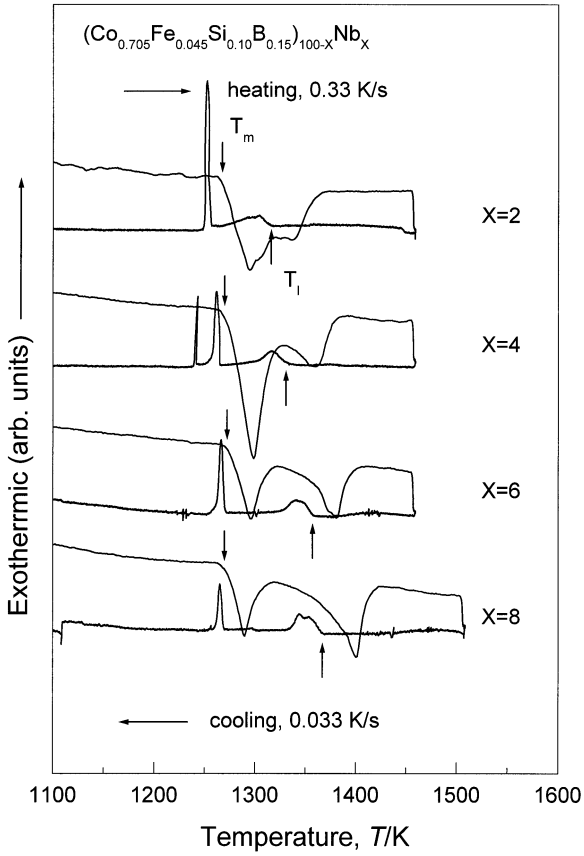

Fig. 2 DTA curves of $(Co_{0.705}Fe_{0.045}Si_{0.1}B_{0.15})_{100-x}Nb_x$ ($x = 2$, 4, 6 and 8 at%) alloys.

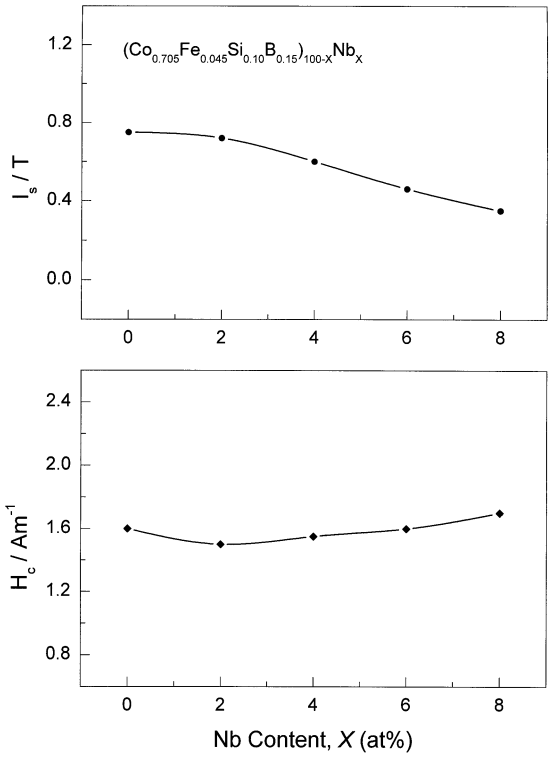

Fig. 3 Saturation magnetic flux density (I_s) and coercive force (H_c) as a function of Nb content for melt-spun $(Co_{0.705}Fe_{0.045}Si_{0.1}B_{0.15})_{100-x}Nb_x$ amorphous alloy ribbons.

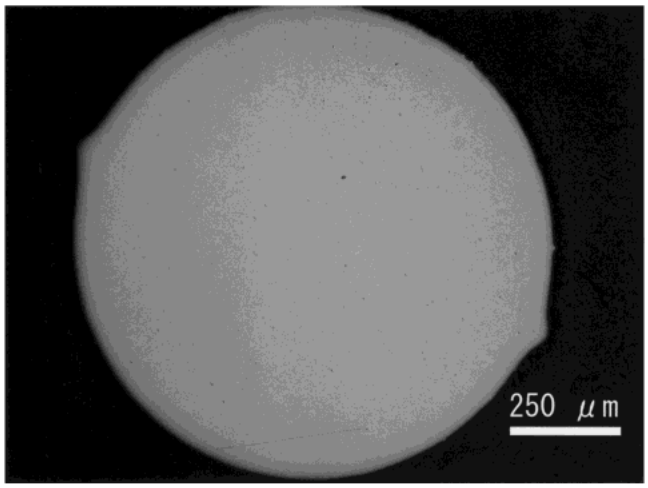

Fig. 4 Optical micrograph of the transverse cross section of the cast $(Co_{0.705}Fe_{0.045}Si_{0.1}B_{0.15})_{96}Nb_4$ glassy alloy rod with a diameters of 1 mm.

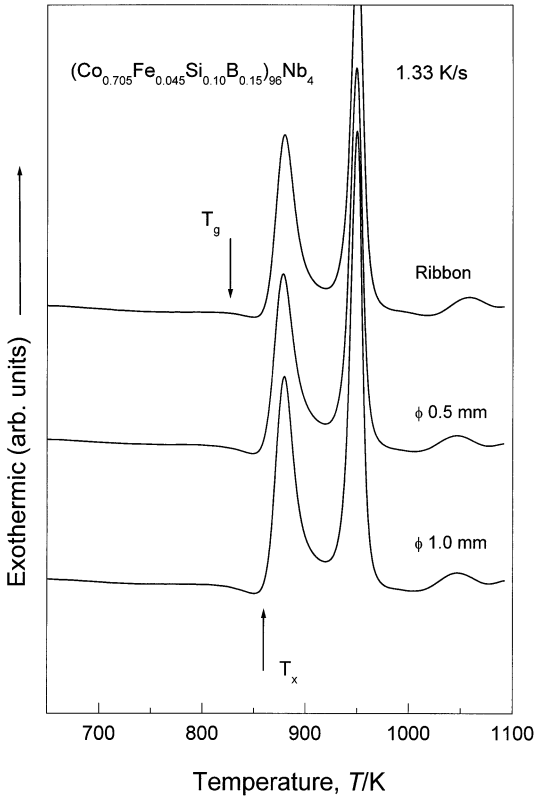

Fig. 5 DSC curves of the cast $(Co_{0.705}Fe_{0.045}Si_{0.1}B_{0.15})_{96}Nb_4$ glassy alloy rods with diameters of 0.5 and 1 mm. The data of the corresponding melt-spun glassy alloy ribbon are also shown for comparison.

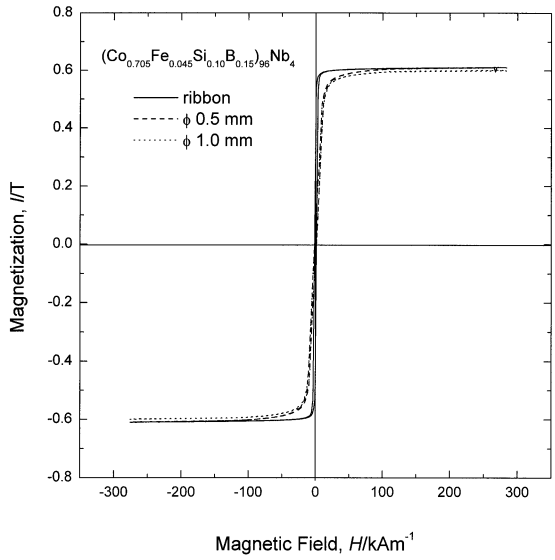

Fig. 6 Hysteresis I–H loops of the cast $(Co_{0.705}Fe_{0.045}Si_{0.1}B_{0.15})_{96}Nb_4$ glassy alloy rods with diameters of 0.5 and 1 mm. The data of the corresponding melt-spun glassy alloy ribbon are also shown for comparison.

ference in the endothermic reaction due to the glass transition and the exothermic reaction due to crystallization between the ribbon and the cast rod samples. From the metallographic data shown in Fig. 4 and the thermal stability data shown in Fig. 5, it is concluded that the cast Co-based alloy rods have a glassy phase without appreciable crystalline phase in the diameter range up to 1 mm. Figure 6 shows the hysteresis I–H loops of the cast Co-based alloy rods with diameters of 0.5 and 1 mm, together with the data of the melt-spun glassy alloy ribbon. The hysteresis B–H loops of bulk samples were measured only by VSM because the conventional B–H loop tracer could not be used for the cylindrical form of the bulk glassy alloys. The cast alloy rods have I_s of 0.59 T and very low H_c below 3 A/m. The I_s and H_c are nearly the same as those for the corresponding melt-spun glassy alloy ribbon. The lower initial permeability resulting from the slight tilt in the I–H loop is seen only for the rod samples, in agreement with the previous data for the cast ferromagnetic alloy rods in Fe–(Al, Ga)–(P, C, B),[11] Fe–(Zr, Hf, Nb)–B[15] and Co–Fe–Ta–B[10] systems. The lower initial permeability for the rod samples has been thought to be an apparent phenomenon including the influence of a demagnetizing field

Table 1 Thermal stability and magnetic properties of the cast $(Co_{0.705}Fe_{0.045}Si_{0.1}B_{0.15})_{96}Nb_4$ glassy rods with diameters of 0.5 and 1 mm. The data of the melt-spun glassy ribbon are also shown for comparison.

	I_s/T	H_c/Am^{-1}	T_g/K	ΔT_x/K	T_g/T_l
Ribbon	0.60	1.55	823	38	0.61
ϕ0.5 mm	0.60	<3	823	38	0.61
ϕ1.0 mm	0.59	<3	823	38	0.61

caused by the rod shape.[10,11,15] Table 1 summarizes the thermal stability and magnetic properties of the cast Co-based alloy rods with diameters of 0.5 and 1 mm. The data of the melt-spun glassy alloy ribbon are also shown for comparison. The H_c of the melt-spun glassy alloy ribbon was measured with an I–H loop tracer. All the thermal stability and soft magnetic properties are independent of the sample thickness. It is thus concluded that Co-based bulk glassy alloys with good soft magnetic properties can be formed in the diameter range up to 1 mm at the composition of $(Co_{0.705}Fe_{0.045}Si_{0.1}B_{0.15})_{96}Nb_4$ by copper mold casting.

4. Discussion

It was found that the addition of 4 at%Nb to $Co_{70.5}Fe_{4.5}Si_{10}B_{15}$ alloy enabled us to form bulk glassy alloy rods with a diameter up to 1 mm by copper mold casting. The previous data on the maximum thickness for formation of an amorphous phase in Co–Fe–Si–B alloys indicate that its maximum value is dependent on preparation method, *i.e.*, 20 μm by using the ordinary melt spinning method and 160 μm by use of the instantaneous stop method of rapidly rotating copper wheel within 1 to 2 seconds.[26] In any event, it is clearly concluded that the glass-forming ability of the Co–Fe–Si–B alloys is significantly enhanced by the addition of 4 at%Nb through the appearance of the glass transition phenomenon and the increase in the reduced glass transition temperature to 0.61. We discuss the reason for the effectiveness of Nb addition on the increase in thermal stability of supercooled liquid as well as the enhancement of glass-forming ability. We have previously proposed that bulk glassy alloys with diameters above several millimeters are formed in the alloys which satisfy the following three criteria,[23–25] *i.e.*, (1) multicomponent consisting of more than three elements, (2) significantly different atomic size mismatches above about 12% among the main three constituent elements, and (3) suitable negative heats of mixing among the main three elements. Although the Co–Fe–Si–B alloys are composed of the four elements, the previous concept on the bulk glassy alloy components consisting of three different type of elements, as exemplified for Fe–(Al, G)–(P, C, B),[9] Fe–(Zr, Hf, Nb)–B,[15] Fe–Co–Ln–B,[17] Fe–(Cr, Mo)–(P, B, C)[19] and (Co, Fe)–Ta–B,[10] indicates that the Co–Si–B alloys consist only of two different types of elements as presented by (Co, Fe)–(Si, B). This result indicates the necessity of the third additional element for the formation of a bulk glassy alloy in (Co, Fe)–(Si, B) system. The addition of Nb to (Co, Fe)–(Si, B) alloys leads to the atomic size mismatches of 14% for Nb/Co, 22% Nb/Si, 59% for Nb/B, in addition to the significant atomic size mismatches of 7% for Co/Si and 39% for Co/B.[27] Furthermore, all the heats of mixing for Nb–Co, Nb–Si and Nb–B pairs as well as Co–Si and Co–B pairs are negative and the absolute values are in the range of 33 to 79 kJ/mol.[28] The satisfaction of the three component rules for the formation of bulk glassy alloys and the stabilization of supercooled liquid by the addition of Nb to Co–Fe–Si–B alloys is the reason for the formation of bulk glassy Co–Fe–Si–B–Nb alloy rods, though the maximum sample thickness is limited to up to 1 mm. The success of forming the Co–Fe–Si–B base bulk glassy alloys which are important as engineering magnetic materials is expected to affect great effect on the future development of soft magnetic materials.

5. Summary

We examined the possibility of forming a bulk glassy Co-based alloy in Co–Fe–Si–B system by the addition of Nb which leads to the satisfaction of the three component rules for formation of bulk glassy alloys. The results obtained are summarized as follows.

(1) Although no glass transition was observed for the $(Co_{0.705}Fe_{0.045}Si_{0.1}B_{0.15})_{100-x}Nb_x$ ($x = 0$ and 2 at%), the addition of more than 4 at%Nb caused the appearance of glass transition and supercooled liquid region before crystallization. The T_g, T_x, ΔT_x and T_l increase with increasing Nb content and the ΔT_x and T_g/T_l values are 38 K and 0.61, respectively, for the 4%Nb alloy and 40 K and 0.64, respectively, for the 8%Nb alloy.

(2) The bulk glassy alloy rods with diameters up to 1 mm were produced for the 4%Nb alloy by copper mold casting. The bulk glassy alloy rods with diameters of 0.5 and 1 mm exhibit the T_g of 823 K, ΔT_x of 38 K and T_g/T_l of 0.61 which agree with those for the corresponding melt-spun glassy alloy ribbon.

(3) The bulk glassy alloy rods also exhibit good soft magnetic properties of about 0.6 T for I_s and low H_c below 3 A/m which is nearly the same as those for the glassy alloy ribbon.

(4) The reason for the significant improvement of glass-forming ability of the Co–Fe–Si–B base alloys was interpreted to be attributed to the satisfaction of the three component rules caused by the Nb addition. The synthesis of the Co–Fe–Si–B base bulk glassy alloy rods is promising for bright future of soft magnetic bulk materials.

REFERENCES

1) A. Inoue, T. Zhang and T. Masumoto: Mater. Trans., JIM **30** (1989) 965–972.
2) A. Inoue, K. Ohtera, K. Kita and T. Masumoto: Jpn. J. Appl. Phys. **27** (1988) L2248–L2251.
3) A. Inoue, T. Zhang and T. Masumoto: Mater. Trans., JIM **31** (1990) 177–183.
4) A. Peker and W. L. Johnson: Appl. Phys. Lett. **63** (1993) 2342–2344.
5) A. Inoue: Mater. Sci. Forum **312–314** (1999) 307–314.
6) A. Inoue, N. Nishiyama and T. Matsuda: Mater. Trans., JIM **37** (1996) 181–184.
7) X. M. Wang, I. Yoshii, A. Inoue, Y. H. Kim and I. B. Kim: Mater. Trans., JIM **40** (1999) 1130–1136.
8) A. Inoue, T. Zhang, W. Zhang and K. Kurosaka: Acta Mater. **49** (2001) 2645–2652.
9) A. Inoue and G. S. Gook: Mater. Trans., JIM **36** (1995) 1180–1183.
10) B. L. Shen, H. Koshiba, A. Inoue, H. M. Kimura and T. Mizushima:

Mater. Trans. **42** (2001) 2136–2139.
11) A. Inoue, Y. Shinohara and G. S. Gook: Mater. Trans., JIM **36** (1995) 1427–1433.
12) B. L. Shen, H. Koshiba, T. Mizushima and A. Inoue: Mater. Trans., JIM **41** (2000) 873–876.
13) T. D. Shen and R. B. Schwarz: Appl. Phys. Lett. **75** (1999) 49–51.
14) B. L. Shen, H. Koshiba, H. M. Kimura and A. Inoue: Mater. Trans., JIM **41** (2000) 1478–1481.
15) A. Inoue, T. Zhang, T. Itoi and A. Takeuchi: Mater. Trans., JIM **38** (1997) 359–362.
16) A. Inoue, T. Zhang and A. Takeuchi: Appl. Phys. Lett. **71** (1997) 464–466.
17) W. Zhang and A. Inoue: Mater. Trans., JIM **42** (2001) 1835–1838.
18) X. M. Wang, I. Yoshii and A. Inoue: Mater. Trans., JIM **41** (2000) 539–542.
19) S. Pang, T. Zhang, K. Asami and A. Inoue: Mater. Trans. **42** (2001) 376–379.
20) T. D. Shen and R. B. Schwarz: Acta Mater. **49** (2001) 837–847.
21) A. Inoue and B. L. Shen: Mater. Trans. **43** (2002) (in press).
22) T. Itoi and A. Inoue: Mater. Trans. **41** (2000) 1256–1262.
23) A. Inoue: Mater. Trans., JIM **36** (1995) 866–875.
24) A. Inoue: Acta Mater. **48** (2000) 279–306.
25) A. Inoue: Mater. Sci. Eng. **A304–306** (2001) 1–10.
26) M. Hagiwara, A. Inoue and T. Masumoto: Sci. Rep. Res. Inst. Tohoku Univ. **A29** (1981) 351–358.
27) *Metals Databook*, ed. by Japan Inst. Metals, Maruzen, Tokyo (198) p. 8.
28) F. R. Niessen: *Cohesion in Metals*, (Elsevier Science Publishers, Amsterdam, 1988) pp. 224–225.